Trans. Japan Soc. Aero. Space Sci.
Vol. 68, No. 1, pp. 12–18, 2025
DOI: 10.2322/tjsass.68.12

Experimental Investigation on Ionization Length Required for Efficient Operation of Argon Hall Thrusters*

Dibyesh SATPATHY,[1)†] Hokuto SEKINE,[1)] Nadine BARTH,[2)] Rei KAWASHIMA,[3)]
Kimiya KOMURASAKI,[1)] and Hiroyuki KOIZUMI[4)]

[1)]*Department of Aeronautics and Astronautics, The University of Tokyo, Tokyo 113–8656, Japan*
[2)]*Faculty of Aerospace Engineering and Geodesy, University of Stuttgart, Stuttgart 70569, Germany*
[3)]*Department of Electrical Engineering, Shibaura Institute of Technology, Tokyo 135–8548, Japan*
[4)]*Department of Advanced Energy, The University of Tokyo, Kashiwa, Chiba 277–8561, Japan*

The propellant utilization efficiency of RAIJIN-66, a 2-kW class Hall thruster with anode layer, was investigated with varying anode temperature to evaluate ionization length, which is the length of the ionization region determined by the channel and magnetic field design. During RAIJIN-66's thermally transient operation from the ignition, the ion beam current was monitored as a function of anode temperature using an ion collector plate biased negatively at 40 V. Two magnetic field profiles were examined with and without trim yokes. From the measured correlation between the propellant utilization efficiency and anode temperature, the ionization length was evaluated. As a result, the ionization length was 5.6 mm without the yokes, and 2.5 mm with the yokes. The ionization length of 2.5 mm was enough to achieve high propellant utilization efficiency with xenon, while it is too short to operate with argon because argon ionization mean free path is notably longer than xenon. This measured length was experimentally confirmed to be almost independent of discharge voltage and electron temperature. In conclusion, to achieve the high performance with argon propellant equivalent to that with xenon propellant, the ionization length as long as 14.5 mm is required in RAIJIN-66 size thrusters.

Key Words: Thruster with Anode Layer, RAIJIN, Alternative Propellant, Anode Cooling, Magnetic Configuration Design

Nomenclature

A_c: cross-section area of the channel, m^2
A_m: total area of manifold walls, m^2
e: elementary charge, C
I_b: ion beam current, A
k_B: Boltzmann constant, Nm/K
L_i: ionization length, mm
m: mass, kg
$\dot{m}_A$: anode mass flow rate, kg/s
n: number density, $1/m^3$
N_A: Avogadro number
P: pressure, Pa
R: gas constant, J/kg·K
T: temperature, K
v: particle velocity, m/s
V_D: discharge voltage, V
z: axial position, m
Z_w: collision frequency per unit area, $s^{-1}\cdot m^{-2}$
α: ratio of $k_B T_e / eV_D$
σ_i: ionization cross-section, m^2
η_u: propellant utilization efficiency
λ_i: ionization mean free path, mm
$\Delta\varphi_i$: potential drop in ionization region, V

Subscripts
e: electron
i: ion
n: neutral
z: coordinate along the thruster axis

*Received 1 October 2023; final revision received 27 April 2024; accepted for publication 13 June 2024.
†Corresponding author, dibyeshsatpathy@g.ecc.u-tokyo.ac.jp

1. Introduction

Due to its outstanding suitability for both smaller satellites and bigger spacecraft, Hall thrusters have become more desirable for use in space applications. In recent years, the market for a reliable yet cost-effective propulsion system for space applications has been increasing rapidly. As a result, there has been an in-depth exploration of electric propulsion systems, specifically Hall thrusters. There are two main variants of Hall thrusters: the Stationary Plasma Thrusters (SPT) and the Thrusters with Anode Layers (TAL).[1)] TAL features a shorter acceleration zone surrounded by metal guard-rings, biased at the cathode potential, and propellant gas is fed through a hollow anode. There are a few basic differences between SPT and TAL, but TAL has a higher thrust density than SPT. With the smaller channel, there is less contact area with ions; channel erosion is reduced, and this supports the long-term operation of the thruster. It also offers significantly greater technical possibilities, particularly in the high-power operation regime.[2)]

The exploration of alternative propellants has been on the rise due to the escalating cost of xenon propellant. The low ionization energy needs of krypton and iodine have led to them being regarded as potential substitutes. However, it has been difficult to get them for experimental uses due to their exorbitant cost or toxicity. Argon, oxygen, and water have also been tested as abundant propellants.[3–6] SpaceX flew their argon Hall thruster, demonstrating that an argon propellant system can be applied to space missions. Argon has a relatively higher ionization potential than other propellants like xenon and krypton. Nonetheless, its lower atomic mass also results in higher neutral gas velocity and lower performance compared to xenon and krypton. With an increase in neutral velocity, the neutral residence time becomes shorter than the ionization time, and hence the ionization fraction becomes poor.

The performance of a Hall thruster is highly dependent on neutral velocity. To estimate it, the neutral gas temperature has been assumed to be equal to the temperature of the channel walls or anode for the SPT or TAL variants respectively. Reid et al.'s[7] numerical calculations show that cooling the anode lowers the axial velocity of the neutrals at the anode outlet for anode temperatures ranging from 300 to 1100 K. The axial velocity's square root dependency on anode temperature was also demonstrated in those simulations, suggesting that the anode temperature is the main determinant of the neutral gas velocity. Huang et al.'s[8] Laser-Induced Fluorescence (LIF) studies showed that the flow regime is transitional and that heating, and ionization processes have a significant impact on Hall thruster neutral flow. For varied discharge voltage settings, Book et al.[9] tested the thrust performance for cooled and uncooled anode cases. They stated that in the case of a cooled anode case compared to an uncooled anode, the thrust was greater under low discharge voltage circumstances. By accumulating the discharge current on a different anode band positioned below the gas distributor, Martinez et al.[10] could eliminate the primary heating mechanism for the anode gas distributor. Because the injection velocity was lower due to the lower gas distributor temperature, the neutral residence time was longer for the given channel length. According to Li et al.'s[11] PIC simulations, when the anode temperature rises, the neutral density decreases, and this is followed by a drop in the frequency of electron-neutral collisions and a drop in the mobility of electrons caused by collisions inside the channel. Satpathy et al.[12] showed real-time thrust measurement and demonstrated a decrease in thrust performance with anode temperature, under low discharge voltage condition xenon operation. Under the low discharge voltage condition, the electron temperature is low, making vigorous ionization of the propellant impossible. Thus, when the anode temperature rises, the neutral density decreases, which deteriorates the propellant utilization efficiency and, eventually, the thruster performance.

In this study, a TAL, known as RAIJIN-66, a downscaled version of RAIJIN-94,[13] was used to examine the relationship between anode temperature and performance with argon propellant. Due to its lower mass, neutral velocity is already high, and with increasing temperature, performance is expected to change more significantly. This paper reports the association between anode temperature and propellant utilization efficiency and evaluates the sensitivity of ionization parameters on anode temperature.

2. Theoretical Description

2.1. Relation between ionization parameters and propellant utilization efficiency

In Hall thrusters, the association between propellant utilization efficiency and ionization parameters is given using a simplified zero-dimensional model as[12]

$$\begin{aligned}\eta_u &= \frac{I_b m_i}{e\dot{m}_A} \\ &= 1 - \exp\left(\frac{-L_i}{\lambda_i}\right) \\ &= 1 - \exp\left(\frac{-L_i(n_e\langle\sigma_i v_e\rangle)}{v_{nz}}\right),\end{aligned} \tag{1}$$

where, I_b is the beam current, m_i is the atomic mass of the propellant gas, $\dot{m}_A$ is the anode mass flow rate, L_i is the ionization length determined by the thickness of the high magnetic flux density region in the channel, λ_i is the ionization mean free path of the neutral particles, $\langle\sigma_i v_e\rangle$ is the ionization rate coefficient. The rate coefficient versus electron temperature is shown in Fig. 1 (top), using the ionization cross-section data. The neutral axial flow velocity v_{nz} is given as

$$v_{nz} = \frac{1}{4}v_n = \frac{1}{4}\sqrt{\frac{8k_B T_n}{\pi m_i}}. \tag{2}$$

Here, k_B, v_n and T_n is the Boltzmann constant, the average particle velocity, and the temperature of neutral particles, respectively. The ionization mean free path is shown in Fig. 1 (bottom). The electron temperature is considered as

$$T_e = \alpha V_D. \tag{3}$$

Here, T_e is the electron temperature and V_D is the discharge voltage. α is a proportionality constant assuming electron temperature scales linearly with discharge voltage. This has been considered as 10% of discharge voltage in this study, although values ranging from 4.4% to 12% of discharge voltage have been considered in previous studies.[14,15] Electron density can be estimated by assuming the quasi-neutral condition, $n_e \approx n_i$ and the ion density can be estimated[16] by using fluid approximation:

$$n_e = n_i = \frac{I_b}{e v_i A_c}, \tag{4}$$

$$I_b = \eta_u\frac{e\dot{m}_A}{m_i}, \quad v_i = \sqrt{\frac{2e\Delta\varphi_i}{m_i}}. \tag{5}$$

Here, I_b and v_i are the beam current measured by the ion collector and ion velocity, respectively. v_i is estimated at the channel exit using the potential drop $\Delta\varphi_i$ in the ionization region. Then the electron density in the ionization region can be taken as:

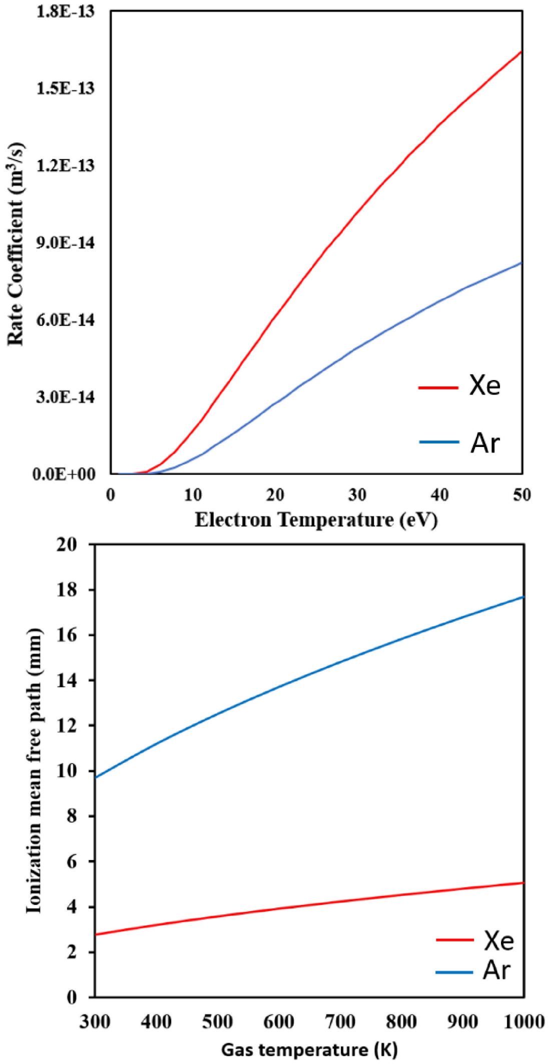

Fig. 1. Ionization rate coefficients for xenon and argon[18] (top), ionization mean free for xenon and argon (bottom).

$$n_e = \frac{\eta_u \dot{m}_A}{A_c\sqrt{2em_i\Delta\varphi_i}}. \tag{6}$$

The neutral particle density can be given as

$$n_n = \frac{\dot{m}_A}{m_i A_c v_n}. \tag{7}$$

In TAL thrusters, the propellant gas is assumed to fully accommodate the temperature of the anode. This essentially leads to an increase in the thermal velocity of the gas with anode temperature. The increase in thermal velocity of the neutral particle results in a decay in neutral residence time, resulting in poor ionization due to the fast neutrals escaping the ionization region before an ionization event. For efficient operation of Hall thrusters,[17] ionization length L_i should be longer than the ionization mean free path λ_i. When the ratio of ionization length to ionization mean free path is 1, the propellant utilization efficiency is to be 63%, and to achieve more than 95% efficiency the ratio must be higher than 3 as calculated using Eq. (1).

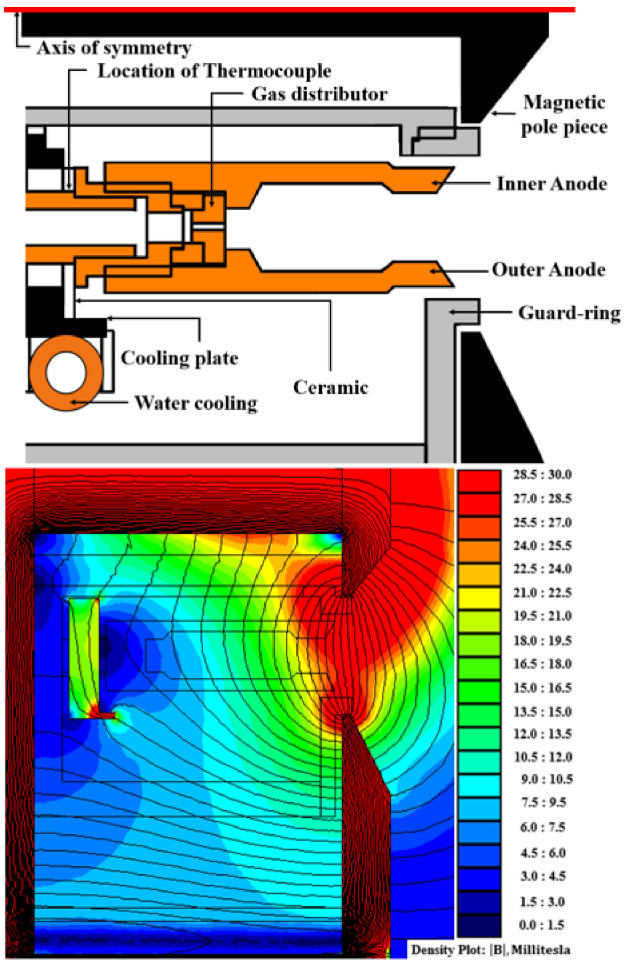

Fig. 2. Cross-section of RAIJIN-66 (top), without trim yokes (bottom).

2.2. Ionization length in RAIJIN-66 with two magnetic field configurations

In the RAIJIN-66's default magnetic design, magnetic shielding (MS) configuration is enabled through the presence of trim yokes (TY). The magnetic shielding configuration is effective in eliminating ion loss to the guard-rings by acceleration region shifting.[19] In this configuration, the ionization region is present downstream of the channel which leads to limited bombardment of ions on the guard-ring. In the configuration with no trim yoke, the ionization region is expanded upstream of the channel, and this configuration ensures that there is a wider magnetic field for the fast argon neutrals to ionize. Figure 2 shows the cross-section of RAIJIN-66 and the magnetic field line distributions without trim yokes.

The ionization length is assumed to end at the exit of the guard-rings where the neutral particle density discontinuously decreases because of diffusion into vacuum. Hence, if the axial distribution of the magnetic flux density is known, the ionization length can be determined. During xenon operation with magnetic shielding, a short ionization is expected. In the case of no magnetic yokes, the length of the ionization region is large due to a broader magnetic field distribution, and it includes a channel length of 2.1 mm (for RAIJIN-66). The starting position of the ionization length

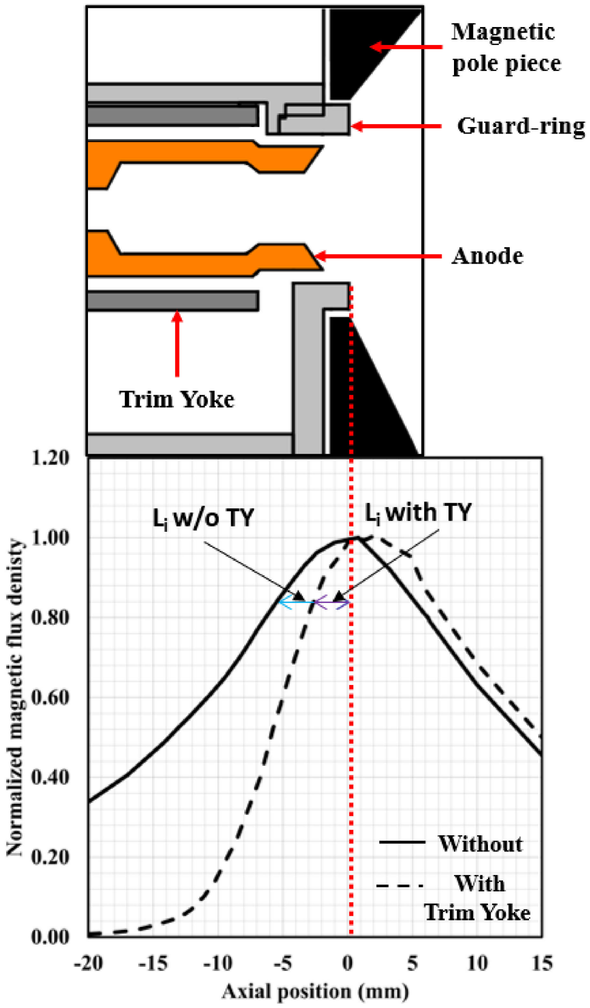

Fig. 3. Axial distribution of normalized magnetic flux density.

is in the anode, and the specific location depends on the specific value of the ionization length. Specific values of the length of ionization can be estimated based on operational parameters: the gas thermal velocity, electron number density, electron temperature, and performance parameters like thrust or propellant utilization efficiency, which will be elaborated in the next section. The ionization length with the two magnetic field configurations for RAIJIN-66 is shown in Fig. 3. It shows $L_{\rm i}$ can be doubled by removing the trim yoke.

The ionization length $L_{\rm i}$ can be deduced from the curve fitting of measured propellant utilization for the no-trim yoke case (this work) and for the trim yoke case as described later. The oscillation amplitude in TAL in the case of no magnetic shielding case is expected to be more significant as compared to the case with magnetic shielding, as reported by Yokota et al.,[20] where a very similar study as of this present investigation was used to evaluate ionization oscillations and reported that the thruster efficiency increases when operated with xenon. However, with argon, it was found that the ionization length would be too small for proper operation to begin with in the case of with-trim yoke, and hence all experiments in this study are conducted without trim yoke.

3. Experimental Setup

All experiments were conducted in a stainless-steel cylindrical vacuum chamber of 2 m in diameter by 3 m in length using 99.99% argon, evacuated using a diffusion pump (PFL-36, ULVAC) with a pumping speed of 37,000 l/s, backed by two rotary pumps (PKS-070, ULVAC) with pumping speed of 250 l/s each and one mechanical booster pump (PMB-060B, ULVAC) with pumping speed of 10,000 $\mathrm{m^3/h}$. The minimum pressure can decrease to 1.2×10^{-4} Pa, without introducing the gas. The pressure was measured using a GL-D7 ionization gauge. Subsequently, the gas flow is controlled using two mass flow controllers (MODEL 3200, KOFLOC) for the thruster and one (MODEL 3660, KOFLOC) for the cathode. The hollow cathode used in this study was manufactured by Plasma Controls, LLC, and 20 SCCM of argon is supplied to the cathode during operation. In all the experiments, 60 SCCM of argon was supplied to the anode, and the backpressure during the operation was 5.3×10^{-3} Pa.

In RAIJIN-66, since the anode is made of copper, a uniform temperature encompassing it can be anticipated because of its excellent thermal conductivity. To measure the anode temperature, a K-type direct contact thermocouple is attached to the anode, as shown in Fig. 2 (top). Although there can be a temperature difference of about 70 K from the anode tip to the anode base, the neutral gas temperature is assumed to be fully accommodated to the anode base (manifold) temperature due to the high number of collisions in the manifold in this study. The 70 K difference is due to the thermal resistance of the copper anode, and since the cross-sectional area of the copper is constant, the slope is also constant. Although the gas is gradually heated in the anode wall, its effect is outside the scope of this zero-dimensional analysis. The number of collisions with manifold wall can be quantified using collision frequency per unit area as

$$Z_{\rm w} = \frac{1}{4} \cdot \frac{N_{\rm A} \cdot P}{RT_{\rm n}}. \tag{8}$$

Here, $N_{\rm A}$ is the Avogadro number and P is the pressure in the manifold. For continuum-based conditions in the manifold,[7] pressure can be represented as

$$P = 1.4 \frac{\dot{m}_{\rm A}}{A_{\rm m}} \sqrt{RT_{\rm n}}, \tag{9}$$

where $A_{\rm m}$ represents the area of manifold walls. Through Eq. (8) and Eq. (9), collision frequency per unit area is approximated as $1.1 \times 10^{18}\ \mathrm{s^{-1}{\cdot}m^{-2}}$ at RAIJIN-66's manifold when neutral gas temperature is 500 K. As such, the temperature of neutral gas is expected to be the same as the measured anode base temperature. To measure the anode temperature dependency during the thermally transient operation of the thruster, all the measurements were started with the anode temperature brought back to approximately 300 K by water cooling. For the measurement of the ion beam current, a collector plate with dimensions 50 cm × 50 cm and 0.1 cm thickness was used. Assuming a symmetric ion beam, a quar-

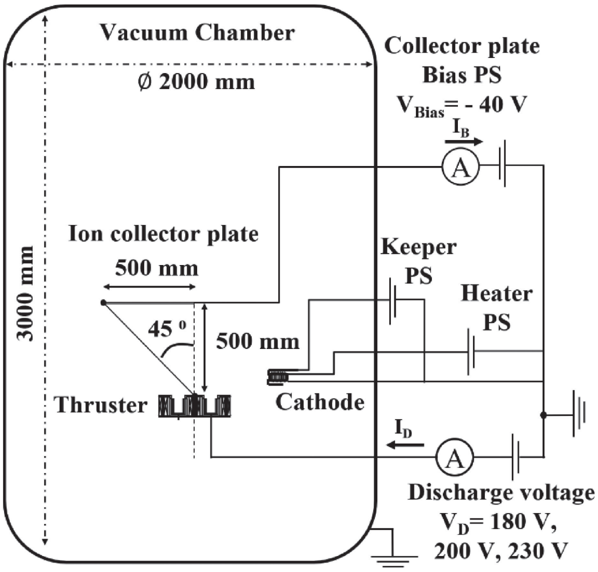

Fig. 4. Electrical schematic of the experiment setup.

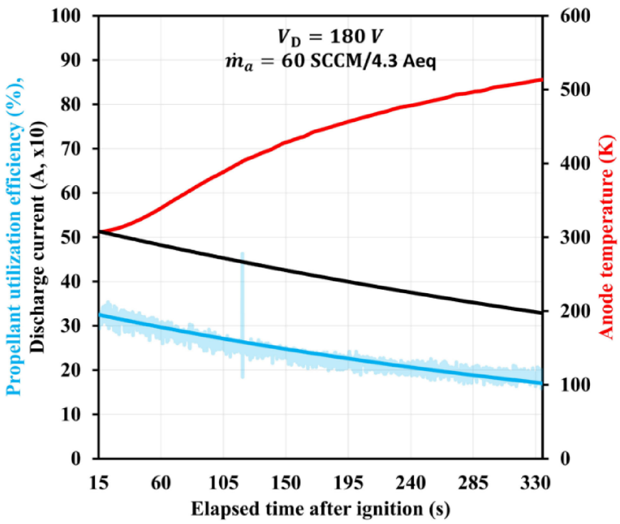

Fig. 5. Measurements for discharge voltage 180 V.

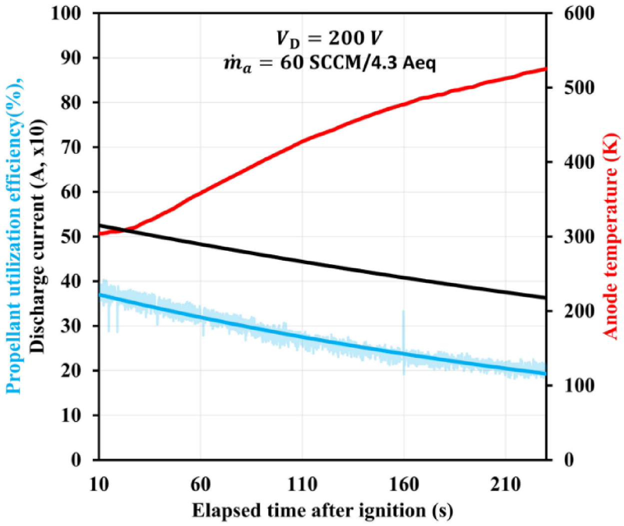

Fig. 6. Measurements for discharge voltage 200 V.

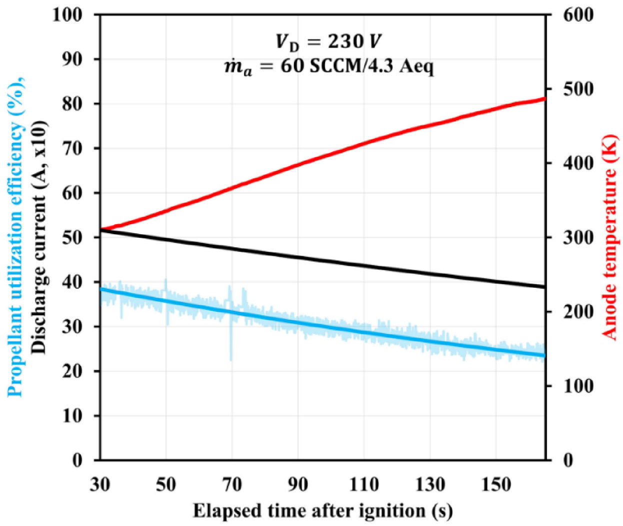

Fig. 7. Measurements for discharge voltage 230 V.

ter of the beam inside the divergence angle of about ±45 deg was collected by this plate. This plate was biased at a negative potential of 40 V to repel any incoming electrons. The collected beam current is multiplied by 4 to get the total plume area. The propellant utilization efficiency is calculated from the measured ion current using Eq. (1). It was found through previous experiments that this approach for measurement shows a close match when ion beam current is measured using a Faraday Probe.[21] Three different discharge voltage cases were investigated based on fixed anode flow rate. Figure 4 shows the electrical schematic and the scale of the collector plate to RAIJIN-66.

4. Experimental Results

4.1. Transient operation at $V_D = 180$ V

An experiment was conducted for more than 5.5 minutes with a discharge voltage of 180 V. Figure 5 shows the measurement with a discharge voltage condition of 180 V. During operation, the discharge current reduced from 5.1 A to 3.4 A. As the anode temperature increases from 308.15 K to 485.15 K, the propellant utilization efficiency reduces from 33% to 17%.

4.2. Transient operation at $V_D = 200$ V

An experiment with a 200 V discharge voltage is run for around 4 minutes. Figure 6 shows the measurement with a discharge voltage condition of 200 V. A decrease in a discharge current from 5.3 A to 3.6 A occurs. Propellant utilization efficiency decreases from 36.2% to 19.7% when the anode temperature rises from 304 K to around 529.75 K.

4.3. Transient operation at $V_D = 230$ V

An experiment with a discharge voltage of 230 V was run for approximately three minutes, during which the discharge current decreased from 5.3 A to 3.9 A. Figure 7 shows the measurements with a discharge voltage condition of 230 V. When the temperature rises from 310 K to 493 K, the propellant utilization efficiency drops from around 38.1% to approximately 23.6%.

5. Discussion

5.1. Ionization length deduced from the slope of propellant utilization efficiency

Figure 8 shows the measured and theoretical propellant utilization efficiencies using Eq. (1). General trend of voltage utilization efficiency with various discharge voltages can be found in literature.[17,22] A value of 85% has been opted for curve fitting, considering a minimal change in voltage utilization efficiency from 180 V to 230 V. Although $\Delta\varphi_i$ and T_e will change with discharge voltage they alter the slope $\Delta\eta_u/\Delta T_n$, very little. The slope strongly depends solely on L_i. This fitting showed higher sensitivity to anode temperature than as shown in our previous study,[12] where the electron density was assumed unchanged with operating conditions. Here, L_i is assumed as a design parameter determined by the geometry of magnetic coils and pole pieces and independent of operating conditions. In fact, L_i was found to be independent of the discharge voltage in the curve fitting of Fig. 8.

5.2. Performance comparison with xenon

In our previous study,[12] the correlation between propellant utilization efficiency and anode temperature with xenon was deduced from the real-time thrust measurements using a thruster with trim yokes, in which the ionization length was estimated to be 1.1 mm. In contrast, trim yokes were removed in this study to increase the ionization length for argon propellant operation. However, this estimation assumed the ratio of electron temperature and discharge to be voltage 0.1 and electron density as 10^{18} m^{-3}, which is likely an overestimation. When electron density was recalculated using Eq. (6), the ionization length was found to be 2.5 mm as shown in Fig. 9. Here, the mean ion acceleration voltage is taken as 80% of discharge voltage (low discharge voltage operation). As the anode temperature increases from 357 K to 402 K, the propellant utilization efficiency decreases from 75.3% to 69.7%. On a comparative basis, the decay in performance for xenon is small compared to argon. This is because argon has a lower atomic mass than xenon, which signifies higher neutral velocity than xenon. Due to the increase in anode temperature, the neutral particle velocity increases further, so decay is more prominent for argon. Table 1 shows the required ionization length to achieve high propellant utilization efficiency with argon propellant in RAIJIN-66. To achieve the propellant utilization efficiency comparable to xenon at 400 K, the L_i should be larger than the ionization mean free path of argon at the same gas temperature, that is, L_i must be as long as 14.5 mm. As it can be established that the ionization length is nearly independent of voltage and electron temperature, the influence of gas species on ionization length estimation is negligibly small.

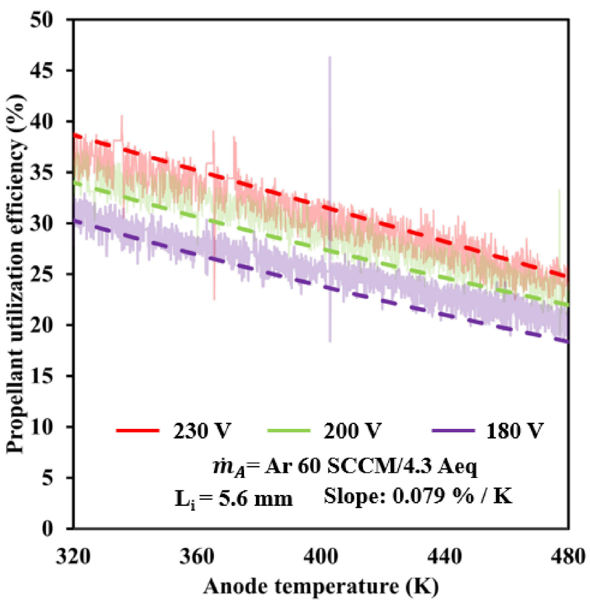

Fig. 8. Measured and theoretical propellant utilization efficiencies. The solid lines show the measured efficiency, while the dashed lines show the theoretical efficiency. The ionization length L_i is deduced from the slope.

6. Conclusion

This study investigates the ionization length required for the efficient operation of Hall thrusters with argon propellant. Three cases were investigated based on discharge voltage

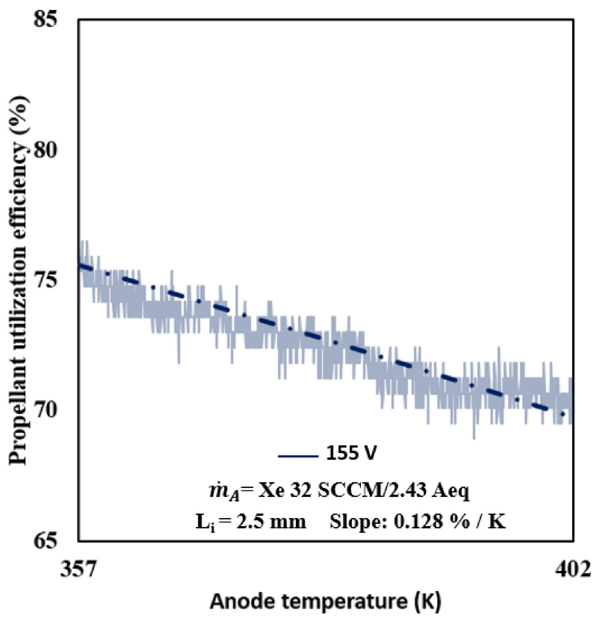

Fig. 9. Propellant utilization efficiency for xenon. The ionization length L_i is deduced from the slope.

Table 1. Required ionization length for argon in RAIJIN-66 whose channel width is 12 mm.

η_u	Required L_i	
	T_n = 400 K	T_n = 800 K
63%	12.3 mm	17.4 mm
86%	24.3 mm	34.5 mm
95%	37.1 mm	52.5 mm

conditions of 180 V, 200 V, and 230 V at a fixed flow rate of 60 SCCM. It was found that decay in performance with anode temperature is significantly more prominent in the case of argon than xenon, with propellant utilization efficiency decreasing from 38.1% to 23.6% when anode temperature increased from 310 K to 493 K, when the discharge voltage was 230 V.

Based on curve fittings to the measured correlation between the propellant utilization efficiency and anode temperature, the ionization length was estimated to be 5.6 mm without the magnetic yoke. In this process, the ionization length was found to be the fitting slope, and it was confirmed to be almost independent of discharge voltage. This ionization length was significantly shorter than the ionization mean free path of argon, which led to poor ionization. The ionization mean free path of the neutral particle was verified to be proportional to its thermal velocity, which was estimated through the measurement of anode temperature. To achieve a propellant utilization efficiency of 63%, the ionization length must be approximately 12.3 mm when the propellant gas temperature is 400 K.

Propellant utilization efficiency is expected to increase with the ionization length by redesigning the thruster and incorporating a flatter magnetic flux density distribution than the current RAIJIN-66. Active cooling would be quite attractive, especially for argon Hall thrusters to achieve high propellant utilization.

Acknowledgments

The work was supported by the JSPS KAKENHI (Grant No. 24KJ0766) from the Japan Society of Promotion of Science.

References

1) Choueiri, E. Y.: Fundamental Difference between the Two Hall Thruster Variants, *Phys. Plasmas*, **8** (2001), pp. 5025–5033.
2) Keidar, M. and Isak, B.: *Plasma Engineering: Applications from Aerospace to Bio and Nanotechnology*, Academic Press, U.S., 2013, pp. 286–288.
3) Komurasaki, K. and Arakawa, Y.: Hall Current Ion-thruster Performance, *J. Propuls. Power*, **8** (1992), pp. 1212–1216.
4) Fujita, D., Kawashima, R., Ito, I., Akagi, S., Suzuki, J., Schönherr, T., Koizumi, H., and Komurasaki, K.: Operating Parameters and Oscillation Characteristics of an Anode-layer Hall Thruster with Argon Propellant, *Vacuum*, **110** (2014), pp. 159–164.
5) Nakagawa, T., Yamamoto, N., Komurasaki, K., and Arakawa, Y.: Experimental Investigation of a Hall Thruster Using Oxygen as the Propellant, *J. Jpn. Soc. Aeronaut. Space Sci.*, **51** (2003), pp. 606–612. (in Japanese)
6) Shirasu, K., Kuwabara, H., Matsuura, M., Koizumi, H., Nakagawa, Y., Watanabe, H., Sekine, H., and Komurasaki, K.: Demonstration and Experimental Characteristics of a Water-vapor Hall Thruster, *J. Electric Propulsion*, **2** (2023), 11.
7) Reid, B. M. and Gallimore, A. D.: Review of Hall Thruster Neutral Flow Dynamics, IEPC-paper, IEPC-038, 2007.
8) Huang, W., Gallimore, A. D., and Hofer, R. R.: Neutral Flow Evolution in a Six-kilowatt Hall Thruster, *J. Propuls. Power*, **27** (2011), pp. 553–563.
9) Book, C. F. and Walker, M. L. R.: Effect of Anode Temperature on Hall Thruster Performance, *J. Propuls. Power*, **26** (2010), pp. 1036–1044.
10) Martinez, R. A. and Walker, M. L. R.: Propellant Thermal Management Effect on Neutral Residence Time in Low-voltage Hall Thrusters, *J. Propuls. Power*, **29** (2013), pp. 528–539.
11) Li, H., Li, X., Zhiyong, G. A., Yongjie, D., Liqiu, W. E., Daren, Y. U., and Xiaogang, W. A.: Particle-in-cell Simulation for Effect of Anode Temperature on Discharge Characteristics of a Hall Effect Thruster, *Plasma Sci. Technol.*, **20** (2018), 125504.
12) Satpathy, D., Kawabata, S., Sekine, H., Kawashima, R., Komurasaki, K., and Koizumi, H.: Investigation of Correlation between Thrust and Anode Temperature during Transient Operation of RAIJIN-66, *J. Electric Propulsion*, **2** (2023), 5.
13) Hamada, Y., Kawashima, R., Bak, J., Komurasaki, K., and Koizumi, H.: Characterization of Acceleration Zone Shifting in an Anode-layer-type Hall Thruster RAIJIN66, *Vacuum*, **186** (2021), 110040.
14) Shagayda, A. A.: On Scaling of Hall Effect Thrusters, *IEEE Trans. Plasma Sci.*, **43** (2014), pp. 12–28.
15) Dannenmayer, K. and Mazouffre, S.: Elementary Scaling Relations for Hall Effect Thrusters, *J. Propuls. Power*, **27**, 1 (2011), pp. 236–245.
16) Shagaida, A. A., Gorshkov, O. A., and Tomilin, D. A.: Influence of the Erosion of the Discharge Channel Wall on the Efficiency of a Stationary Plasma Thruster, *Tech. Phys.*, **57** (2012), pp. 1083–1089.
17) Goebel, D. M. and Katz, I.: *Fundamentals of Electric Propulsion: Ion and Hall Thrusters*, John Wiley & Sons, U.S., 2008, pp. 334–337.
18) Hagelaar, G. J. M. and Pitchford, L. C.: Solving the Boltzmann Equation to Obtain Electron Transport Coefficients and Rate Coefficients for Fluid Models, *Plasma Sources Sci. Technol.*, **14** (2005), pp. 722–733.
19) Kawashima, R., Hamada, Y., Kawabata, S., Komurasaki, K., and Koizumi, H.: Wall Ion Loss Reduction by Acceleration Zone Shifting in Anode-Layer Hall Thruster, *J. Propuls. Power*, **38** (2022), pp. 489–493.
20) Yokota, S., Takahashi, D., Cho, S., Kaneko, R., Hosoda, M., Komurasaki, K., and Arakawa, Y.: Magnetic Topology to Stabilize Ionization Oscillation in Anode-layer-type Hall Thruster, *Trans. JSASS Aero. Tech. Jpn.*, **10**, ists28 (2012), pp. Pb_31–Pb_35.
21) Bak, J., Loo, B. V., Kawashima, R., and Komurasaki, K.: Discharge Characteristics and Increased Electron Current during Azimuthally Nonuniform Propellant Supply in an Anode Layer Hall Thruster, *J. Appl. Phys.*, **128** (2020), 023302.
22) Ross, J. L.: Probe Studies of a Hall Thruster at Low Voltages, Ph.D. Diss., Mich. Tech. Uni., 2011.

Yasushi Ohkawa
Associate Editor